THERMAL ANALYSIS OF ROAD TUNNELS

Buonsanti M.
Researcher – University of Reggio Calabria – michele.buonsanti@unirc.it
Leonardi G.
Associate Professor - University of Reggio Calabria – giovanni.leonardi@unirc.it
Scopelliti F.
Researcher – University of Reggio Calabria – francesco.scopelliti@unirc.it

ABSTRACT

Fire accidents in underground road tunnels lead to temperature histories characterized by high heating rates and temperatures exceeding 1000°C. This situation results in severe damage of concrete linings as observed during recent fire accidents in European tunnels.

This work presents a thermal model to analyse the behaviour under high-temperature of the structure of road tunnels.

In particular, the study investigates the temperature distribution inside a 3d model of Zillastro tunnel (Italy) and the effects of different fire-load scenarios on the materials and structure.

Keywords: tunnels, fire, fem, safety

1.   INTRODUCTION

In Europe there are about 7 thousand kilometres of tunnel and 27% of these are in Italy, where approximately 1/3 is constituted by road tunnels (639 kilometres) with three great alpine and one apennine tunnels: Great Saint Bernard, Mount Blanc, Freyus and Gran Sasso.

The larger part of accidents that occur in road tunnels is always followed by the development of a fire.

The fire inside tunnels and underground transportation facilities is one of the more catastrophic events that can occur during the transport of goods and people.

The high temperatures, the minimal possibility of escape and the impossibility of smoke and heat elimination makes this type of fire very dangerous and its cost, in terms of human lives and economic loss, is extremely high, as, unfortunately, demonstrated by the latest tragic episodes that took place in Europe.

In the last 10 years fires of great dimensions inside road and railway tunnels have taken place and have caused an impressive number of deaths and enormous economic losses.

The particular structure of a tunnel makes the fight against the fire extremely complex, above all because of the limited possibilities of escape, the difficulties of rescue services and the intense heat that there is in this situation of limited thermal dispersion. Life is threatened by asphyxiation, poisoning and generation of high temperatures, and by the spalling action of concrete which may block escape routes and cause injury during an incident to the escaping public and to the fire and rescue services.

The structural stability of the tunnel lining may also be compromised because of:

- A major loss of concrete lining thickness due to explosive spalling as a result of the thermal shock following a rapid rise in temperature during the early stages of a fire.
- A reduction in the strength of the concrete when its temperature exceeds 380ºC for long periods.
- A reduction in the strength of the steel reinforcement when its temperature exceeds 250ºC.
- Damage or destruction of the tunnel joints and seals, leading to water leakage and possible failure of an immersed tube construction.

By the economic point of view, moreover, the damages of a fire in a tunnel are often of enormous dimensions because loss of revenue associated with long tunnel closures, together with costs of repairs may total hundreds of millions of euro, also prolonged closure of the tunnel will result in major traffic diversions, possible overloading of the local road network and environmental damage.

So, one of the main problems of a tunnel construction regards its fire structural resistance. The fire that develops in a tunnel, in fact, generates a thermal attack to the materials used for the construction of the tunnel that cannot be compared to what happens in the other civil buildings.

So in this paper, we want to study by a finite element analysis the effect that a temperature stress of elevated intensity and extended in the time has on the structure of

a tunnel; in particular the application regards the "*Traforo dello Zillastro*", a tunnel of next realization 6 km long.

We analyze the efficiency of the coating protection layer to apply to the ceilings of the tunnel, simulating the thermal attack in order to estimate the performance of the structure.

2.   FIRE RESISTENCE OF ROAD TUNNELS

Fire protection in tunnels and underground transportation facilities is argument of study of numerous experts of the field.

So in recent years a great deal of international researches has been developed to ascertain the types of fire which could occur in tunnel and underground spaces. This research has taken place in both real, disused tunnels and laboratory conditions.

As a consequence of the data obtained from these tests, a series of time/temperature curves for the various exposures have been proposed as detailed in figure 1.
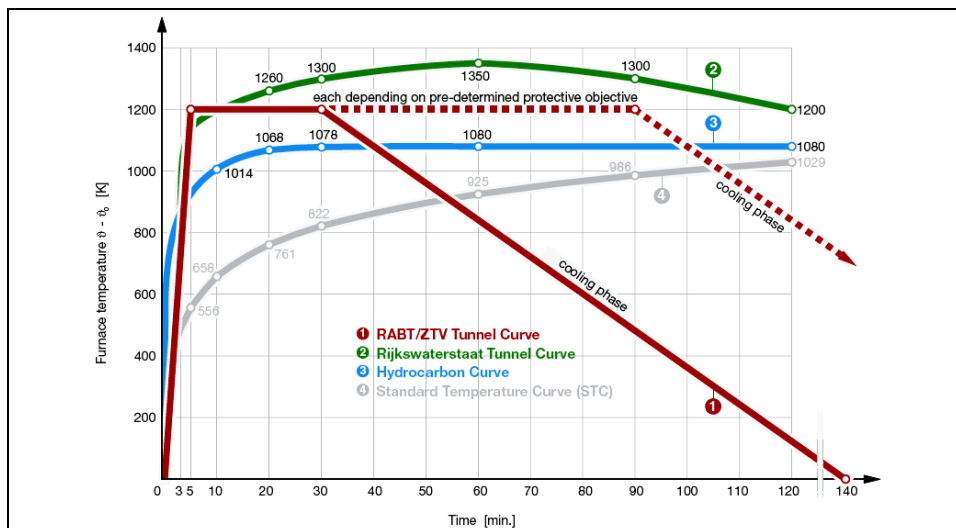

Figure 1 Tunnel fire curves [Cafco 2006)]

Standard fire tests to which specimens of constructions subject to are based on the use of the Cellulosic time/temperature curve ISO 834, as defined in various national standards [Gottfried (2007)]. This curve is based on the burning rate of the materials found in general building materials and contents:

$$\theta_g = 20 + 345 \log_{10} (8t + 1)$$

It is general opinion that ISO 834 is a bad representative of a real fire, that has a completely different behaviour, but its use can give acceptable indications about the resistance of the materials in the times after the flash over. Equally it is obvious that the

ISO 834 curve is completely unfit to verify the inside structural behaviour of the tunnels.

In order to investigate in more adequate way the materials to use for the protection of the tunnels structures the Rijkswaterstaat, Ministry of Transport in the Netherlands, has proposed the RWS curve.

This curve is based on the assumption that in the worst case scenario, 50 m³ fuels, oil or petrol tanker to fire with to fire load of 300MW could occur, lasting up to 120 minutes. The RWS curve was based on the results of testing carried out by TNO in the Netherlands in 1979 (figure 2).

Recently the correctness of the RWS to fire curves as to design to fire curves for road tunnels was reconfirmed in the Full Tests Scales in the Runehamar tunnel in Norway.

In the December of 2003, the UNI norm 11076 *"Modality of test for the study of the behaviour of protective coatings in tunnels and underground spaces, in fire conditions"* was published.

It must be applied when it is necessary to value the behaviour of protection materials covering the concrete ceilings of tunnels and underground transportation facilities (road, railway, subway, etc.) subject to fire risks deriving from means of transport and their contents.
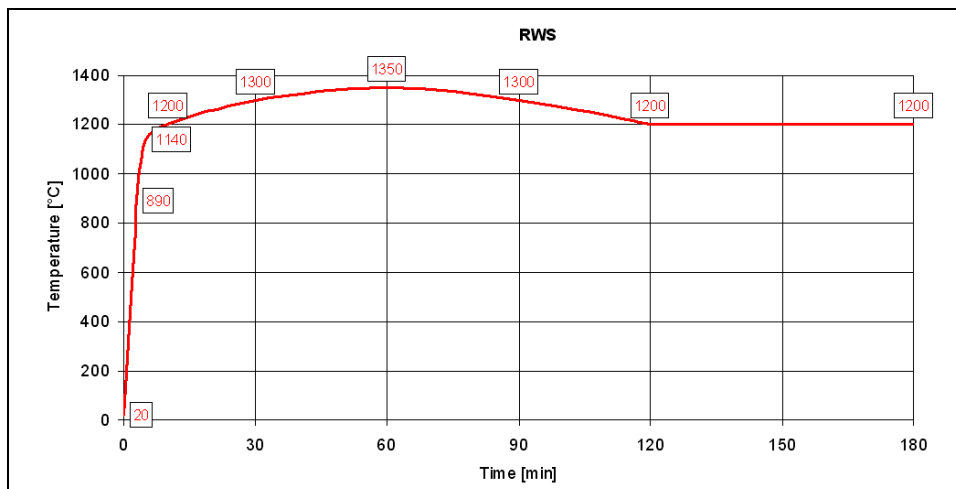

Figure 2 RWS curve

The aim is to verify that the protecting material is able to protect the structure, in such way to guarantee high performances of thermal isolation and to contain, therefore, the rise of the temperature in concrete ceilings avoiding structural collapses caused by the reach of the critical temperature inside the structure that will involve the loss of its carrying capacity (the breaking and the collapse of the concrete ceiling).

The protecting layer will be, therefore, estimated for its capacity to maintain the temperature under the critic one and to reduce or better to contain the damages before the loss of the structural capacity.

As temperature-time curve the RWS curve is used, because this is considered the most representative curve to simulate the development of the fire inside a tunnel.

The temperature development of the RWS fire curve is shown in Figure 1: in the first 5 minutes it grows very quickly, catching up 1140 °C (curve ISO 834 normally used arrives to 576 °C), then continues to grow until the 60 minutes when it catches up the 1350 °C in order to return to 1200 °C after 120 minutes.

The RWS curve simulates the initial rapid growth of a fire using a petroleum tanker as the source, and the gradual drop in temperatures to be expected as the fuel load is burnt off.

The failure criteria for specimens exposed to the RWS time/temperature curve is that the temperature of the interface between the concrete and the fire protective lining should not exceed 380°C and the temperature on the reinforcement should not exceed 250°C.

3.   THERMOMECHANICAL THEORY

Many important stress analysis problems involve structures that are subject to both mechanical and thermal loadings.

Thermal effects, according to Sadd (2005), within an elastic solid produce heat transfer by conduction, and this flow of thermal energy establishes a temperature filed within the material.

Most solids exhibit a volumetric change with temperature variation, and thus the presence of a temperature distribution generally induces stresses create from boundary or internal constraint.

If the temperature variation is sufficiently high, these stresses can reach levels that may lead to structure failure, especially for brittle materials.

The flow of heat in solids is governed by the Fourier law of heat conduction which is the constitutive relation between the heat flux vector q and the temperature gradient ∇T, namely

$$q_i = - \mathbb{K}_{ij} \, T_{,j} \qquad\qquad (Eq. 1)$$

where $\mathbb{K}_{ij}$ is the thermal conductivity tensor. In the isotropic case $\mathbb{K}_{ij} = k \, \delta_{ij}$ and thus

$$q_i = - k \, T_{,j} \qquad\qquad (Eq. 2)$$

where k is the thermal conductivity materials constant and the energetic balance of the system can be written as

$$\rho \mathbf{U} = \sigma_{ij} \, v_{i,j} - q_i + \rho h \qquad\qquad (Eq. 3)$$

Where ρ is the mass density, $\mathbf{U}$ is the internal energy, v_i is the velocity field, and h is any prescribed energy source term.

Considering the Duhamel-Neumann constitutive relation in the isotropic case we have

$$kT_{,ii} = \rho cT + (2\mu + 3\lambda)\, \alpha T^\circ\, \mathbb{E}_{ii} - \rho h \qquad \text{(Eq. 4)}$$

Note that the term $(2\mu + 3\lambda)\, \alpha T^\circ\, \mathbb{E}_{ii}$ involves both thermal and mechanical variables, and this is referred to as the coupling term in the energy equation. It has been shown that for most materials under static or quasi-static loading conditions, this coupling term is small and can be neglected. So, we establish the so-called uncoupled conduction equation

$$kT_{,ii} = \rho cT - \rho h \qquad \text{(Eq. 5)}$$

When it is possible to consider only steady state conditions the (Eq. 5) is reduced as

$$\nabla^2 T = 0 \qquad \text{(Eq. 6)}$$

Let us now formulate the general uncoupled thermo elastic problem by means the follow equations system:

$$\mathbb{E}_{ij} = \tfrac{1}{2}\,(u_{i,j} + u_{j,i}) \qquad \text{(Eq. 7a)}$$

$$\sigma_{ij,j} + f_i = 0 \qquad \text{(Eq. 7b)}$$

$$kT_{,ii} = \rho cT \qquad \text{(Eq. 7c)}$$

The (Eq.s 7a, b, c) represent the fundamental set of field equations for uncoupled thermo elasticity.

Now in plane strain case the basic formulation was given by the displacement field

$$u = u(x,y)\,,\ v = v(x,y)\,,\ z = 0 \qquad \text{(Eq. 8)}$$

so the formulation can be show a reasonable approximation for cylindrical bodies with large z dimension (i.e. longitudinal axis of the tunnel).

In this manner, the following stress field can be formulated

$$\sigma_{ij} = \lambda(u_i + v_j) + 2\mu u_i - \alpha(2\mu+3\lambda)(T - T^\circ) \qquad \text{(Eq. 9)}$$

and, from equilibrium equations we have the formulation in displacement term

$$\mu\nabla^2 + (\lambda+\mu)(u_x + v_y)_I - (2\mu+3\lambda)\alpha\, T_x = 0 \qquad \text{(Eq. 10)}$$

Finally, using Hooke's law

$$\nabla^2(\sigma_x + \sigma_y) + (E\alpha/1 - \nu)\nabla^2 T = 0 \qquad \text{(Eq. 11)}$$

The (Eq. 10) would be used in the displacements formulation while (Eq.11) would be incorporated in the stress formulation.

According to Srinath (1995), we shall now consider the nature of thermal stress induced in a long circular cylinder when the temperature is symmetrical about the longitudinal axis and does not vary along the axis.

If the z axis is the longitudinal axis of the cylinder and r the radius, then T is a function of r alone and it's independent of z.

Since the cylinder is long, section far from the ends can be considered to be in a state of plane strain and so axial displacement u_z assumed to be zero.

After the positions $E^* = E/1-v^2$, $v^*= v / 1-v$, $\alpha^* = (1+v)\alpha$, the constitutive relations follow

$$\mathbb{E}_r =1/E^*(\sigma_r-v^*\sigma_\theta) + \alpha^* T \qquad \text{(Eq. 12a)}$$

$$\mathbb{E}_\theta =1/E^*(\sigma_\theta-v^*\sigma_r) + \alpha^* T \qquad \text{(Eq. 12b)}$$

Consequently the expression for u_r, σ_r, σ_θ, σ_z has the form

$$u_r = (1+v)/(1-v)\alpha 1/r \int_r Trdr + C_1 r + C_2/r \qquad \text{(Eq. 13a)}$$

$$\sigma_r = -[(\alpha E)/(1-v)]1/r^2\int_r Trdr + E/(1+v)[(C_1/(1-2v) + C_2/r^2] \qquad \text{(Eq. 13b)}$$

$$\sigma_\theta = [E/(1-v)]1/r^2\int_r Trdr - \alpha TE/(1-v) + E/(1+v)[(C_1/(1-2v) + C_2/r^2] \qquad \text{(Eq. 13c)}$$

$$\sigma_z = (-\alpha ET/1-v) + 2vEC_1/(1+v)(1-2v) \qquad \text{(Eq. 13d)}$$

The constant C_1 and C_2 are determinated from the boundary conditions.

We shall now consider a particular case about a semicircular hollow tube (figure 3), where the inner surface is a temperature T_i, and the outer surface at a temperature much lower than the inner.
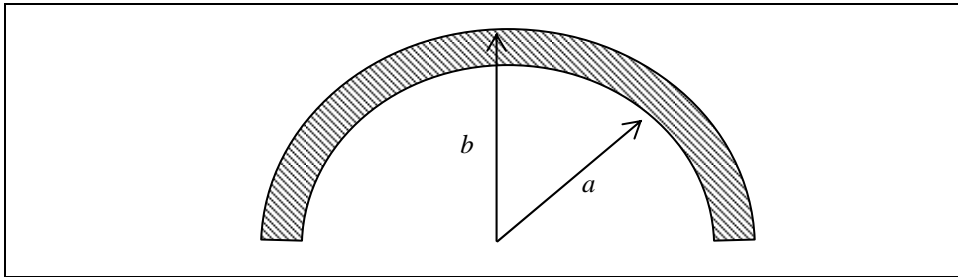

Figure 3 The semicircular hollow cylinder model

Assuming a step with steady state conditions, we put the questions: what are the values of σ_θ and σ_z near the inner and outer surfaces? Under steady heat flow conditions, temperature at any distance r from the centre is given by the expression

$$T = [T_i / log(b/a)] \, log \, (b/r) \qquad \text{(Eq. 14)}$$

The stress components attain their maximum positive and negative values at $r = a$ and $r = b$, and these values are

$$(\sigma_\theta)_{r=a} = (\sigma z)_{r=a} = (\alpha ET_i)/\ 2(1-\nu)log(b/a)\ [1-(2b^2/b^2-a^2)log(b/a)] \qquad \text{(Eq. 15a)}$$

$$(\sigma_\theta)_{r=b} = (\sigma z)_{r=b} = (\alpha ET_i)/\ 2(1-\nu)log(b/a)\ [1-(2a^2/b^2-a^2)log(b/a)] \qquad \text{(Eq. 15b)}$$

If T_i is positive, the radial stress is compressive at all points, whereas σ_θ and σ_z are compressive at the inner surface and tensile at outer surface.

These tensile stress cause cracks in brittle materials such as stone, brick and concrete.

4.   MODELLING OF THE COUPLED PROBLEM

In order to estimate the efficacy of the passive fire protections in road tunnels, an appropriate 3D model of the Zilastro tunnel has been built.

In particular, the behaviour of the structure under the accidental action of a fire has been studied by a particular Finite Element Analysis.

4.1   Thermo-mechanical analysis by finite elements simulation

Our objective in the following section is to discuss the application of the finite element analysis to the solution of thermal and thermo-mechanical problem.

In the study of F.E.A. of heat transfer problems, according to Bathe (1996) it's basilar to first recall the differential and variational equations that govern the heat transfer conditions to be analyzed.

These equations provide the basis for the finite element formulation and solution of the heat transfer problem as well shall then discuss.

Consider a 3-dimensional body in heat transfer conditions and consider, initially, steady state conditions.

For the heat transfer analysis we assume that the material obeys Fourier's law of heat conduction

$$q_i = -\ k_i\ \partial T/\partial i \quad \text{whit } i = x,y,z \qquad \text{(Eq. 16)}$$

here q_i are the heat flows conducted per unit area, T is the temperature of the body B and k_i the thermal conductivities.

For the finite element solution of the heat transfer problem, according to Bathe (1996), we use the principle of virtual temperature

$$\int_B \mathbf{T}'^{\mathrm{T}}\ \boldsymbol{k}\ \mathbf{T}'\ dv = \int_B T^B q^B\ dv + \int_{\partial B} T^{\partial B} q^{\partial B}\ d\partial B + \Sigma_i T_i\ Q_i \qquad \text{(Eq. 17)}$$

where

$$\mathbf{T}'^{\mathrm{T}} = [\ \partial \mathrm{T}/\partial x,\ \partial \mathrm{T}/\partial y,\ \partial \mathrm{T}/\partial z\ ] \qquad \text{(Eq. 18a)}$$

$$k = \begin{bmatrix} k_x & 0 & 0 \\ 0 & k_y & 0 \\ 0 & 0 & k_z \end{bmatrix} \qquad \text{(Eq. 18b)}$$

and Q_i are concentrated heat flow inputs. Each Q_i is equivalent to a surface heat flow input over a very small area.

The principle (Eq. 17) is an equation of heat flow equilibrium and for T to be solution of the temperature in the body, (Eq. 17) must hold for arbitrary virtual temperature distributions such that restraints are respected.

A great variety of boundary conditions are present in this analysis namely, temperature conditions at specific points and surface of B, heat flow conditions, convection boundary conditions, radiation boundary conditions.

The finite elements solution of the heat transfer governing equations is obtained using procedures analogous to those employed in stress analysis.

Assuming that the total body has been idealized as an assemblage of finite elements, then we have at time $t + \Delta t$ for each element e

$$^{t+\Delta t}T^{(e)} = \mathbf{H}^{e(t+\Delta t)} \mathbf{T} \qquad \text{(Eq. 19a)}$$

$$^{t+\Delta t}T^{\partial B(e)} = \mathbf{H}^{\partial B(e)(t+\Delta t)} \mathbf{T} \qquad \text{(Eq. 19b)}$$

$$^{t+\Delta t}\mathbf{T}'^{(e)} = \mathbf{B}^{e(t+\Delta t)} \mathbf{T} \qquad \text{(Eq. 19c)}$$

here $^{t+\Delta t}\mathbf{T}'$ is the vector of all nodal point temperature at time $t + \Delta t$.

The matrices $\mathbf{H}^e$ and $\mathbf{B}^e$ are the elements temperature and temperature-gradient interpolation matrices. Finally we obtain the finite elements governing equations in linear heat transfer analysis in linear steady state conditions case:

$$(\mathbf{K}^k + \mathbf{K}^c)^{\,t+\Delta t}\mathbf{T} = {}^{t+\Delta t}\mathbf{Q} + {}^{t+\Delta t}\mathbf{Q^*} \qquad \text{(Eq. 20)}$$

where $\mathbf{K}^k$ (conductivity matrix) and $\mathbf{K}^c$ (convection matrix) have the form

$$\mathbf{K}^k = \Sigma_e \int_B \mathbf{B}^{e\mathbf{T}} \mathbf{k}^e \mathbf{B}^e \qquad \text{(Eq. 21a)}$$

$$\mathbf{K}^c = \Sigma_e \int_{\partial B} h^e \mathbf{H}^{\partial B(e)\mathbf{T}} \mathbf{H}^{\partial B(e)} \qquad \text{(Eq. 21b)}$$

Finally, let us $^{t+\Delta t}\mathbf{Q^*}$ the vector of a concentrated nodal point heat flow input, then

$$^{t+\Delta t}\mathbf{Q^*} = \Sigma_e \int_{\partial B} h^e \mathbf{H}^{\partial B(e)\mathbf{T}} \mathbf{H}^{\partial B(e)} \mathbf{T} \qquad \text{(Eq. 22)}$$

The above formulation (Eq. 20) and (Eq. 22) is effectively used with the variable-number-nodes isoparametric elements as applied in the next simulation.

4.2   Finite element analysis

A central core of the real tunnel is modelling by means the NASTRAN code (2004). This model has been implemented by solid type-elements to a final mesh as shown in the figure 4.
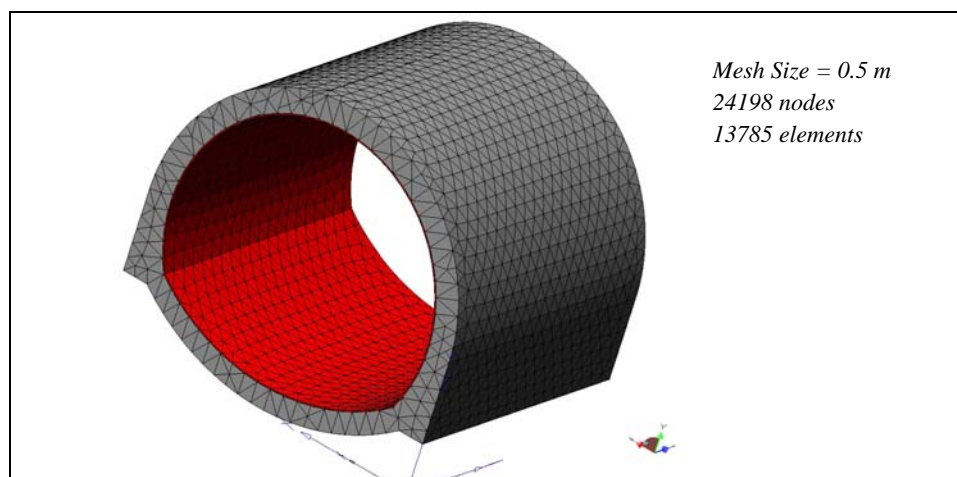

Mesh Size = 0.5 m
24198 nodes
13785 elements

Figure 4 Tunnel partial model and finite element mesh

The considered section is 10m long and it has a difference in level between the axis of the road and the ground elevation of about 300 metres. Moreover, two particular structural configurations have been confronted: the first without passive protection layer and the second with a particular protecting layer 5cm thick and realized with one special plaster pre-mixed thermic insulating made of expanded concrete and vermiculite [Cafco (2007), Campagnoli (2007)].

Table 1 Physical properties of the protecting material [Cafco (2007)]

Characteristic	Tested Performance
Density	704-768 kg/m^3
Combustibility	Noncombustible
Cohesion/Adhesion	354 kPa
Compressive Strength	3778 kPa
Air Erosion Resistance	0.000 g/m^2
Thermal Conductivity	0.19 w/mK @ 24°C
Corrosion Resistance	0.00g/mm^2

Initially two distinct analyses are carried out developing thermal and mechanical analysis in separate manner. Particularly, our attention is focalized in thermal analysis results because, from the comparisons among the models, protection layer effect can be obvious. In the next figure 5 two thermal maps are showed and protection layer effect appear.
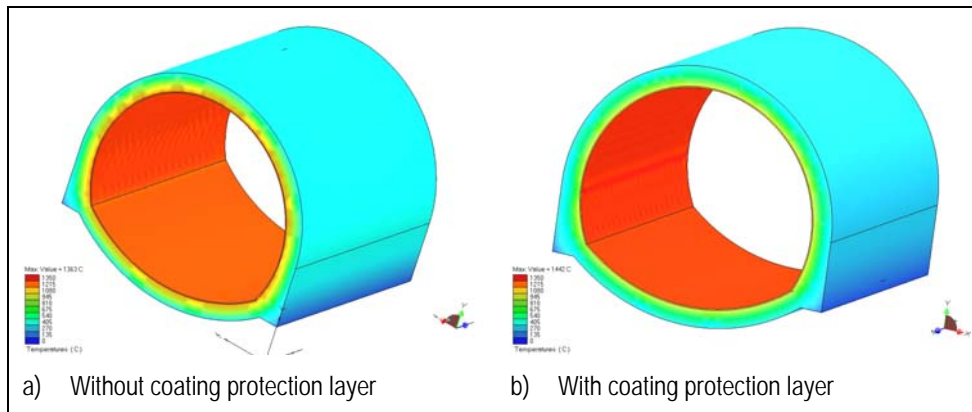
a)   Without coating protection layer   b)   With coating protection layer

Figure 5 Temperature distribution with coating protection layer (1 hour)

On the base of the thermal analysis results, therefore, the distribution of the temperatures inside of the structure is known.
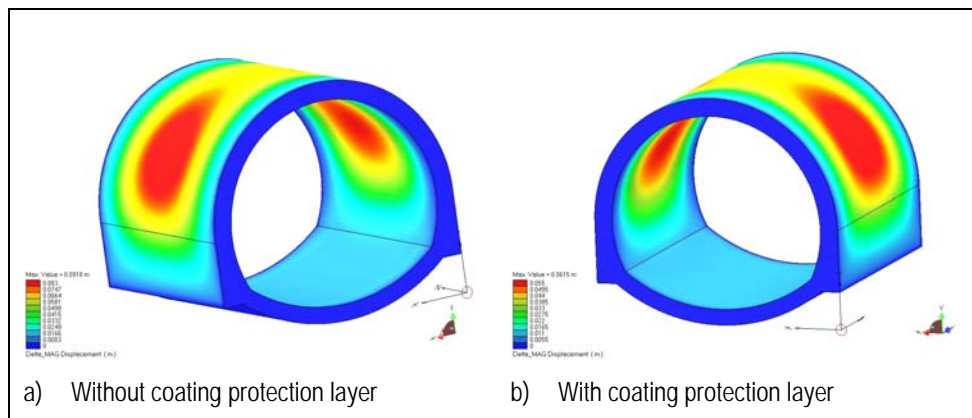

a)   Without coating protection layer   b)   With coating protection layer

Figure 6 Displacement fields

Subsequently, the mechanical behaviour of the two models has been analyzed introducing also to thermal stress, the weights of the structure and of the over ground.

Such analysis is carried out for t = 3600 (1 hour) when we have the greatest thermal stress and when the fire curve assumes the maximum value (1350 °C). The figures 6 and 7 show the displacement and the stress fields.
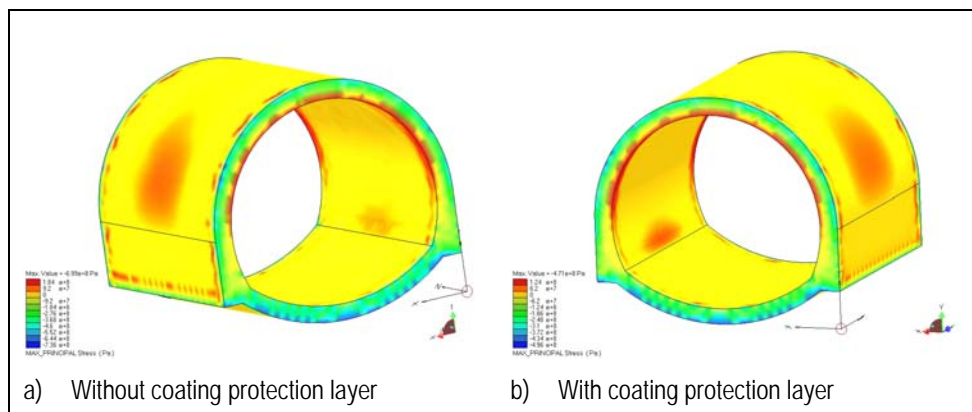
a)   Without coating protection layer   b)   With coating protection layer

Figure 7 Von Mises Stress

If we focalize our attention on strain results (see figure 6) more than figure 8 it's possible to deduce that structural integrity control parameter can be assumed as the deformation field.
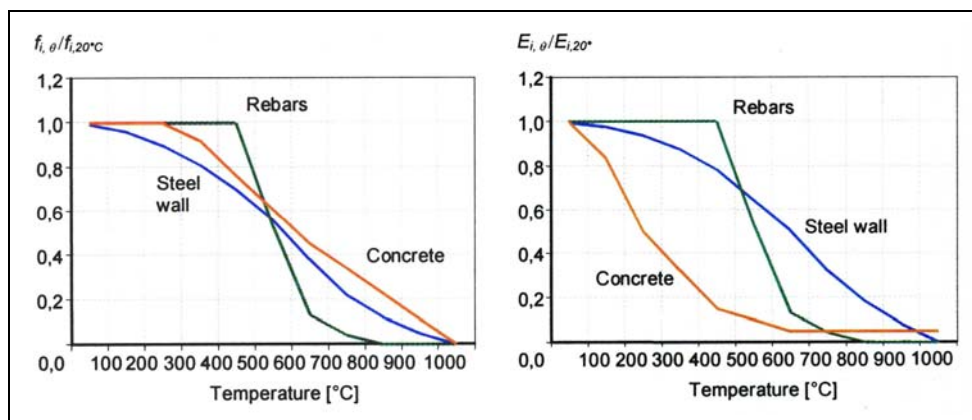

Figure 8 Strength and Stiffness concrete damage under thermal action

This is, because in concrete when temperature up to 300 °C micro fracture appear. In fact the solid is damaged and so the behaviour in evolving time became unstable.

According to Schrefler et al. (2003 and 2002) and Witek et al. (2007) the total effect on the mechanical and thermo-chemical damages acting at same time is multiplicative, namely

$$\mathcal{D} = 1 - [E(T) / E°(T^a)] \qquad \text{(Eq. 23)}$$

Where $E(T)$ is the Young modulus at a given temperature and $E°(T^a)$ is the Young modulus of mechanically undamaged material at room temperature (20°C).

In such conditions concrete may be subject to spalling phenomena which put the integrity of the construction into hazard.

Following the theoretical approach at new problem we go in the dynamic fracture field.

This is the process of fracture in which the inertia effects with the associated wave propagation phenomena are basilar.

According to Bazant we can see fracture as a rate process and focalize the effect of temperature on fracture energy of concrete as well as our initially problem.

Let us $a*$ the amplitude variation of the first fracture then following Bazant we can write the rate equation in the form

$$a* = a_0* \, f \, (K_I / K_{0T}) \qquad \text{(Eq. 24)}$$

where a_0* depends on temperature and has dimensions of velocity, f is dimensionless function, K_I is the stress intensity factor and K_{0T} can also depend on temperature and has dimension equal to K_I.

Now, if we will to consider the effect of temperature on fracture energy of concrete rewrote the (Eq. 24) in the form

$$a* = a_0* \, g \, (G / G_f) \qquad \text{(Eq. 25)}$$

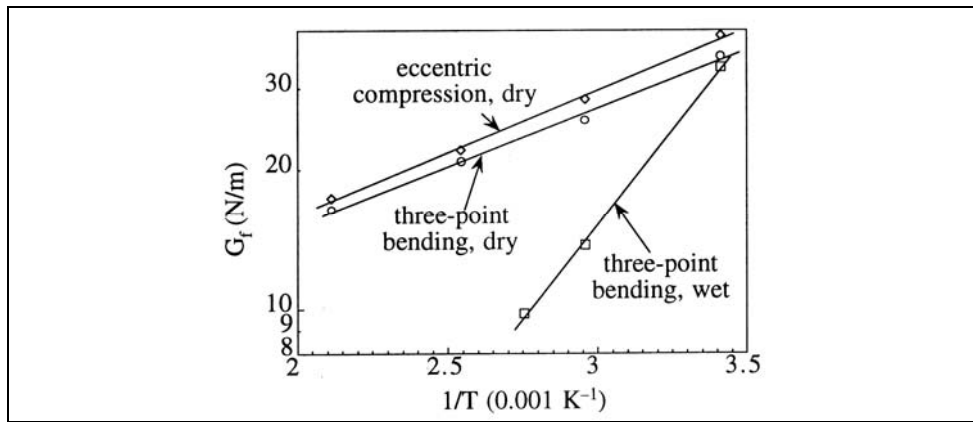where G_f is the fracture energy value at temperature T.

Figure 9 Effects of temperature on fracture energy (from Bazant (1997))

The crack growth rate expression based on T and T° must be equivalent and so

$$G_f = G_f^\circ \, e^{\,(\lambda / T) - (\lambda / T^\circ)} \qquad \text{(Eq. 26)}$$

where λ is constant.

The expression (Eq. 26) represents the value of the fracture energy obtained for each temperature as well as, showed in figure 10 for example, and can be utilized to investigate dynamic propagation of fracture under thermal and mechanical loads.

CONCLUTIONS

The fire disasters over the past few years have shown that fires in tunnels represent high risks. The users and the rescue services are endangered by heat, smoke and concrete spallings of the tunnel lining.

Constructional measures against concrete spalling and structural collapse are of great importance beside reducing the distances rescue services have to cover, the rapid disposal of smoke and dimensioning the structure to cope with the effects of fire.

In this paper, we presented an analysis tool for the assessment of the stability of tunnels under fire load. On the basis of the numerical results obtained from application of this tool to the Zilastro tunnel (Italy), considering two different scenarios: with and without coating protection layer, the temperature the strain and the stress distributions inside the structure were calculated.

The thermal stress simulation showed how a passive fire protective coating works by preventing the temperature of the concrete or steel lining from reaching its critical temperature in fire.

The analysis tool proposed in this paper combines theoretical considerations with a finite element analysis. The proposed 3D structural model and the presented approach of determination of the temperature distribution inside the structure may be readily used for safety assessment of tunnels under fire load.

REFERENCES

CAFCO INTERNATIONAL (2006) - *Passive Fire Protection for Tunnels*.
GOTTFRIED T. (2007) - *Fire Protection in Tunnels and Underground Transportation Facilities* – PROMAT.
SADD M.H. (2005) – *Elasticity* – Elsevier B.H. Academic Press, Amsterdam.
SRINATH L.S.(1995) – *Advanced in Mechanics of Solids* –Tata McGraw Hill, N.Delhi.
BATHE K. J.(1996) – *Finite Element Procedure* – Prentice Hall, U. Saddle River, N.J.
NASTRAN (2004) - *Finite Element Code* – MSC.
CAFCO® (2007) – *Fendolite MII* – Perlite Italiana.
CAMPAGNOLI V. (2007) – *Protezione passiva contro il fuoco di gallerie stradali e ferroviarie* – Strade e Autostrade n. 61.
SCHREFLER B. et al. (2003) - *Modelling of Thermal Damaging of Concrete Structures During Fire*, VII Int. Conf. Computational Plasticity, Onate & Owen Eds. CIMNE.
SCHREFLER, B.A. et al. (2002) - *Concrete at high temperature with application to tunnel fire* - Computational Mechanics 29 (1), pp. 43-51.
WITEK, A., et al. (2007) - *Finite element analysis of various methods for protection of concrete structures against spalling during fire*, Computational Mechanics 39 (3), pp. 271-292.
BAZANT Z.P. (1997) - *Fracture and Size Effect* – CRC Press, New York.